Available online at www.sciencedirect.com

Journal of Catalysis 220 (2003) 358–371

JOURNAL OF CATALYSIS

www.elsevier.com/locate/jcat

NO reduction with ethanol on Pd–Mo/Al_2O_3 catalysts

L.F. de Mello, F.B. Noronha,[1] and M. Schmal *

NUCAT-PEQ-COPPE, Universidade Federal do Rio de Janeiro, Ilha do Fundão, CP 68502, CEP 21941, Rio de Janeiro, Brazil

Received 17 March 2003; revised 10 June 2003; accepted 12 June 2003

Abstract

The NO reduction with ethanol was studied on Pd/Al_2O_3 and Pd–Mo/Al_2O_3 catalysts. The Pd/Al_2O_3 catalyst was more active for NO conversion, although the selectivity for N_2 formation was the same on both catalysts. IR and TPD analysis of adsorbed ethanol showed formation of stable acetate species upon dehydrogenation of ethanol to acetaldehyde at reaction temperature. TPSR measurements suggested that NO preferentially adsorbs on Pd while ethanol selectively adsorbs on alumina and/or partially reduced molybdenum oxide (MoO_x). The catalytic results further suggested that the reaction mechanism was the same on both catalysts and that the reaction occurred between adsorbed NO and acetate species at the metal/oxide interface. A reaction mechanism was proposed where the limiting step was the dehydrogenation of ethanol to acetaldehyde.

© 2003 Elsevier Inc. All rights reserved.

Keywords: Pd–Mo catalysts; TPD of ethanol; IR; NO + ethanol reaction

1. Introduction

Recently, the use of oxygenated organic compounds in gasoline has been growing [1]. The addition of such compounds reduces the emission of olefins, aromatics, complex hidrocarbons, and SO_x. The most commonly used additives are MTBE (methyl *tert*-butyl ether) and alcohols (methanol and ethanol). However, the use of ethanol, for instance, may increase the direct emission of aldehydes (acetaldehyde and formaldehyde) and also of unburned alcohol [2]. Apart from their potential carcinogenic effects, these new emission products may react in the atmosphere to form other toxic compounds and also contribute to the formation of urban smog [3]. Therefore, these facts must be taken into account when projecting and testing catalytic systems with the purpose of automotive pollution control.

Although much work has focused attention on the reduction of NO with several hydrocarbons on various catalysts [1,4], little has been done to determine the effect of the presence of oxygenated organic compounds on the reduction of NO in exhaust gases. Recent papers have called attention to the need for more fundamental research regarding the adsorption properties and reaction mechanistic studies in order to understand and develop adequate catalytic systems. In this sense, Cordi and Falconer [5] studied the oxidation of ethanol and acetaldehyde on alumina-supported palladium catalysts using temperature-programmed desorption (TPD) and oxidation (TPO) while Idriss et al. [6] and Yee et al. [7] studied the reactions of acetaldehyde [6] and ethanol [7] on the surface of CeO_2-supported palladium catalysts also using temperature-programmed desorption and infrared analyses. Ukisu et al. [8] and Miyadera et al. [9] have performed infrared study of the reduction of NO with alcohols on alumina-supported silver catalysts and they have identified the presence of isocyanate species as an important reaction intermediate. Toops et al. [10] studied the NO reduction with methanol over La_2O_3 and they have suggested a mechanism where two types of adsorption sites for methanol and NO were present.

In previous works [11–13], the Pd–Mo system was shown to be very active and selective for N_2 formation during the NO + CO reaction and both the surface characterization and the reduction of NO with CO on Pd–Mo/Al_2O_3 catalysts were thoroughly investigated. For instance, Schmal et al. studied Pd–xMo/Al_2O_3 catalysts, where x indicates the amount of Mo in each catalyst (2, 8, 14, and 20%). The authors performed diffuse reflectance spectroscopy (DRS) and X-ray diffraction (XRD) measurements on the oxidized sam-

---

* Corresponding author.
E-mail addresses: fabiobel@int.gov.br (F.B. Noronha), schmal@peq.coppe.ufrj.br (M. Schmal).

[1] Present address: Instituto Nacional de Tecnologia - INT, Av. Venezuela 82, CEP 20081-310, Rio de Janeiro, Brazil.

0021-9517/$ – see front matter © 2003 Elsevier Inc. All rights reserved.
doi:10.1016/S0021-9517(03)00272-0

ples and the XRD results clearly showed the presence of a crystalline phase (bulk MoO_3) for the samples containing 14 and 20% Mo, while the pattern for the 2% Mo-containing catalyst was similar to that for pure alumina. With the aid of DRS analyses, they showed that for the 8% Mo catalyst a monolayer of octahedrally coordinated molybdenum was the main species present. Schmal et al. [12] and Noronha et al. [13] used temperature-programmed reduction (TPR) experiments on the Pd–Mo catalysts and observed that the Pd–Mo samples presented interesting differences when compared to the Pd-only and Mo-only catalysts, clearly showing an enhancement on the reduction of MoO_3 (lower reduction temperatures) when Pd was present. According to them, this result indicated that Pd facilitates the reduction of molybdenum oxide, thus implying that palladium is in close contact and interacts with the Mo species.

When these catalysts were used for the NO + CO reaction [12], it was found that the presence of Mo enhanced catalytic activity and selectivity for N_2 production. Schmal et al. suggested a redox mechanism to explain the increase in activity and selectivity for these catalytic systems and the intimate contact between Pd particles and MoO_x species would favor this mechanism.

The present paper is a continuation of the same line of work as the previous ones and the main objective here is to study the NO reduction with ethanol on the Pd–Mo catalysts, trying to understand the mechanistic differences between this reaction and the NO + CO reaction, thus giving an integrated view of the Pd–Mo system. For this purpose, the adsorption properties of ethanol and also the reduction of NO with ethanol on Pd–Mo/Al_2O_3 catalysts were investigated using temperature-programmed desorption, temperature-programmed surface reaction (TPSR), and infrared (IR) analyses as well as catalytic activity measurements.

2. Experimental

2.1. Catalyst preparation

The 8%Mo and 20%Mo/Al_2O_3 catalyst were prepared by wet impregnation of γ-Al_2O_3 (Engelhard; BET area = 216 m^2/g) with an aqueous solution of $(NH_4)_6Mo_7O_{24}\cdot 4H_2O$. The samples were dried at 383 K for 22 h and calcined under flowing air at 773 K for 2 h. Pd/Al_2O_3 and Pd–Mo/Al_2O_3 samples were prepared by wet impregnation of Al_2O_3 and Mo/Al_2O_3, respectively, with a 10% nitric acid solution of $Pd(NO_3)_2$ (Aldrich). The samples were then dried at 373 K and calcined under flowing air at 773 K for 2 h. The composition of the catalysts are presented in Table 1.

2.2. Catalyst characterization

2.2.1. Hydrogen chemisorption

The H_2 chemisorption measurements were made on an ASAP 2000C (Micromeritics) equipment. Prior to reduction, the catalysts were dried at 423 K, for 30 min. The samples were then reduced under pure hydrogen (30 cm^3/min) at 773 K (5 K/min) and vacuum was made at the reduction temperature for 1 h followed by cooling to the adsorption temperature. The irreversible adsorption was determined at 343 K according to the method described by Benson et al. [14].

2.2.2. Infrared spectroscopy of adsorbed ethanol

Ethanol adsorption was monitored using a Fourier transform infrared spectrometer (Perkin Elmer 2000). Before the analysis, the catalysts (25 mg pellets) were reduced with H_2 at 773 K for 1 h. After evacuation at the reduction temperature for 1 h and cooling down to room temperature, ethanol uptake was allowed until saturation at 298 K, followed by FTIR measurements under vacuum at 298, 373, 423, 473, 523 and 573 K. For the 20% Mo-containing catalysts, no infrared measurements were made because there was no transmittance through the reduced samples.

An additional infrared measurement was made for the Pd8Mo sample. After the catalyst was reduced (same pretreatments as explained above), the pellet was exposed to a mixture of 7.6 Torr NO/5.0 Torr ethanol initially at room temperature and then raised up to 573 K and cooled to room temperature again. IR measurement were taken before and after heating. A flow of He was passed through the sample and then another measurement was performed. Finally, vacuum was established and IR was taken again.

2.2.3. Temperature-programmed desorption (TPD)

The temperature-programmed desorption experiments of adsorbed ethanol were made in a similar manner as in a previous work [11]. Prior to TPD analyses, all samples were purged under helium flow (50 cm^3/min) from room temperature up to 823 K (10 K/min). The samples were then cooled to room temperature and reduced under flowing H_2 (30 cm^3/min) up to 773 K (5 K/min), remaining at that temperature for 2 h. Following reduction, the system was purged with helium flow at the reduction temperature for 30 min and cooled to room temperature. The adsorption of ethanol was made at room temperature through pulses of an ethanol/He mixture (until saturation), which was obtained by flowing He through a saturator containing ethanol at 298 K. After adsorption, the catalyst was heated at a 20 K/min rate up to 823 K in flowing helium (50 cm^3/min). The products were monitored using a quadrupole mass spectrometer (Balzers, PRISMA).

The calibration of the mass spectrometer as well as the correction procedure to determine the distribution of the desorbed products were described in detail elsewhere [11].

2.2.4. Temperature-programmed surface reaction

The temperature-programmed surface reaction was made following the same procedure as described for TPD analysis. All samples were first purged with helium flow (50 cm^3/min) from room temperature up to 823 K (10 K/min), cooled to room temperature, and reduced under flowing H_2 (30 cm^3/min) up to 773 K (5 K/min), remaining at that temperature for 2 h. After reduction, the system was purged with helium at the reduction temperature for 30 min and cooled to room temperature. Ethanol was adsorbed at room temperature until saturation of the surface. After adsorption, the samples were purged with He and a flow of a 1%NO/He mixture (50 cm^3/min) was passed as the temperature was raised at a 20 K/min rate until 823 K. The reaction products were monitored using a quadrupole mass spectrometer (Balzers, PRISMA), as described before [11].

2.2.5. *Catalytic activity*

The catalytic experiments were performed in a glass microreactor at atmospheric pressure. Prior to the reaction, the catalysts (ca. 140 mg) were pretreated in flowing helium (50 ml/min) at 823 K for 30 min and then reduced with pure H_2 at 773 K for 1 h. The feed mixture for the NO reduction with ethanol consisted of 0.2% ethanol/0.3% NO in He (balance) at a flow rate of 250 ml/min (space velocity = 82,500 h^{-1}). For the reaction gas feed, a 0.97% NO/He (AGA) gas mixture was used while the ethanol/He mixture was obtained by flowing He through a saturator containing 99.999% pure ethanol (Merck) at 278 K. The effluent was analyzed by gas chromatography (Chrompack with TCD detector, Chromosorb 102 column, and cryogen).

3. Results

3.1. *Hydrogen chemisorption*

H_2 chemisorption results are presented in Table 1. The Mo-only catalysts showed virtually no hydrogen chemisorption while for the Pd-containing catalysts there was a drastic decrease in the amount of H_2 chemisorbed as the Mo content increased. This result shows that the presence of MoO_x species reduces the amount of Pd adsorption sites, which in turn may indicate that the molybdenum oxides might be covering the Pd particles. The decoration of Pd particles by the partially reduced molybdenum oxide species was also observed in previous works [12,13] and reported in other papers [15,16]. Konopny et al. [15] have studied the preparation and characterization of alumina-supported Pd–Mo catalysts and observed a similar H_2 chemisorption effect on the bimetallic samples. According to the authors, the reduction of MoO_3 upon exposure to H_2 at high temperatures originates a suboxide that tends to migrate onto the Pd surface, thus preventing its contact with H_2. Due to this effect, the Pd dispersion was calculated only for the Pd/Al_2O_3 and it was found to be 23%. Such low Pd dispersion is usually achieved when palladium nitrate is used as the precursor salt [13].

Table 1
Catalyst composition and H_2 chemisorption

Catalyst	Pd (wt%)	Mo (wt%)	H_2 chemisorption (µmol H_2/g_{cat})
Pd/Al_2O_3	0.69	–	6.64
$8Mo/Al_2O_3$	–	8.3	0.00
$Pd8Mo/Al_2O_3$	0.63	8.3	1.40
$20Mo/Al_2O_3$	–	18.6	0.11
$Pd20Mo/Al_2O_3$	0.60	17.0	0.16

3.2. *Infrared spectroscopy of adsorbed ethanol*

The IR analysis of ethanol adsorption on alumina (Fig. 1) showed characteristic bands of ethoxy species at 1075, 1120, 1168, 1389, and 1447 cm^{-1}. Similar bands were also observed by Greenler [17] after adsorption of ethanol on alumina. The features present at 1585 and 1463 cm^{-1} might be related to the asymmetric and symmetric stretching of acetate species, respectively. In fact, Greenler [17] observed the appearance of such acetate species after heating the alumina surface previously exposed to ethanol. Several reports have also observed the appearance of the above-noted bands related with acetate species upon adsorption of ethanol on different surfaces [6,7,18]. However, in this work, an IR spectrum for the alumina surface without adsorption of ethanol was also taken (not shown) and very weak bands around 1479 and 1586 cm^{-1} were also observed. Although alumina was calcined in flowing air at 773 K for 2 h, it is possible that carbonate species still remained at the surface and originated the bands noted above. Therefore, it is possible that the bands presented in Fig. 1 (1463 and 1585 cm^{-1})

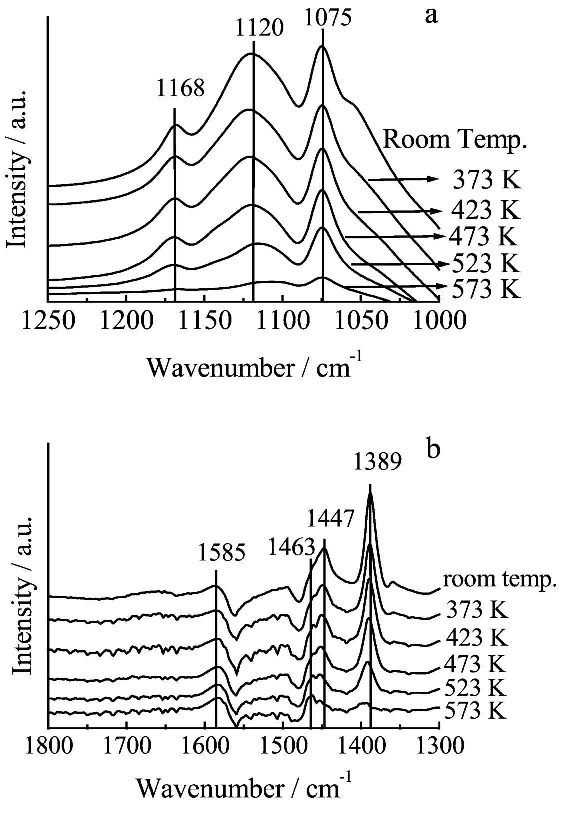

Fig. 1. IR spectra of adsorbed ethanol on Al_2O_3.

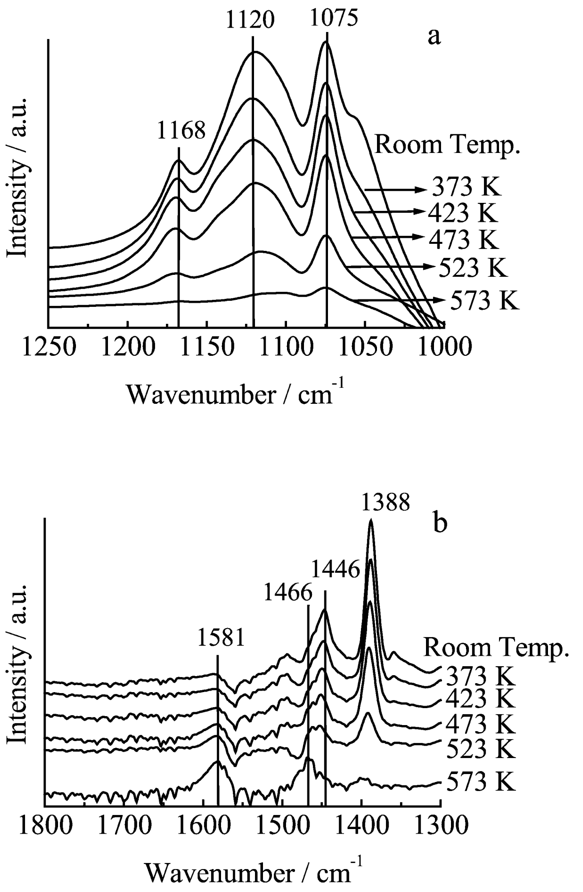

Fig. 2. IR spectra of adsorbed ethanol on Pd/Al_2O_3.

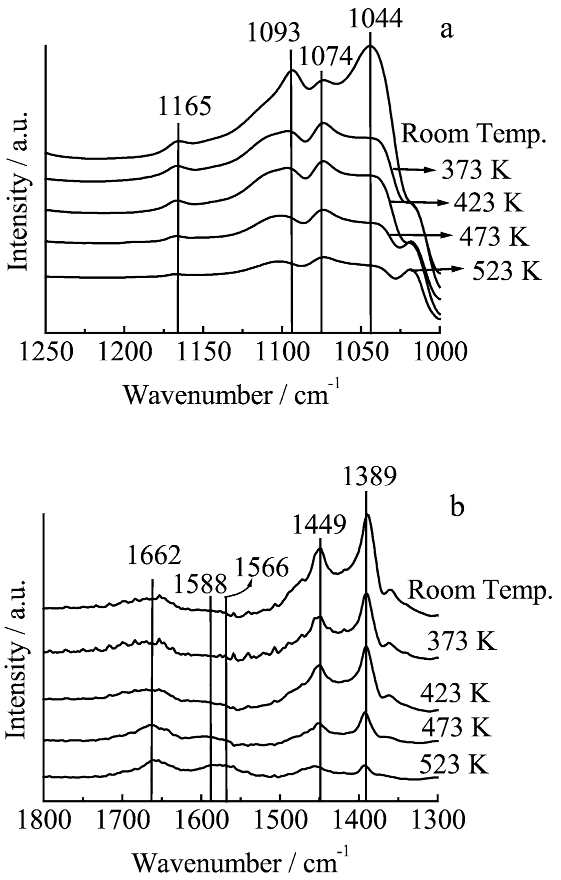

Fig. 3. IR spectra of adsorbed ethanol on 8Mo/Al_2O_3.

are relative to characteristic alumina bands (due to carbonate species) and/or to the presence of acetate species. After heating the sample, the band intensities related to ethoxy species decreased, while those initially related to acetate species were not modified.

The IR spectra of adsorbed ethanol on Pd/Al_2O_3 (Fig. 2) showed, at room temperature, the same bands attributed to ethoxy species on alumina. However, as the temperature was raised, the band intensities of the ethoxy species (1075, 1120, 1168, 1388, and 1446 cm^{-1}) decreased whereas the intensity of the bands related to acetate species (1466 and 1581 cm^{-1}) increased. Such increase in intensity may be associated with the formation of acetate species, suggesting that the presence of Pd favors the appearance of these species.

Figs. 3 and 4 show the IR spectra of ethanol adsorbed on 8Mo and Pd8Mo catalysts. In both cases the bands related to ethoxy species adsorbed on alumina were less intense when compared with the spectra obtained for the support (Fig. 1) and for the Pd/Al_2O_3 catalyst (Fig. 2). This is probably due to the covering of the alumina surface by the MoO_3. A similar effect has been observed in previous works [11,12] and it has also been reported that a monolayer of MoO_3 on alumina is obtained for Mo loadings between 8 and 12% [12,19]. However, new bands around 1044 and 1093 cm^{-1} were observed and are possibly associated with ethoxy species adsorbed on the partially reduced molybdenum oxide (MoO_x). For the adsorption of ethanol on CeO_2-supported Pd catalysts, Yee et al. [7] observed infrared bands at 1037 and 1078 cm^{-1} on reduced cerium oxide and they have also attributed these bands to ethoxy species on the surface of partially reduced cerium oxide.

For the 8Mo catalyst, the bands related to acetate species on alumina (around 1474 and 1587 cm^{-1}) were very weak as the temperature was raised. On the other hand, these bands were very clear on the Pd8Mo catalyst (mainly at 573 K), suggesting, once again, that the presence of Pd favors the formation of such species. On both samples, however, weak bands appeared around 1562–1566 and 1654–1662 cm^{-1}. Although it is not yet clear, these bands are possibly associated with acetate species adsorbed on the surface of partially reduced molybdenum oxide. Infrared analysis of adsorbed acetaldehyde on 8Mo and Pd8Mo (not shown here) presented similar bands in this region after heating, suggesting that acetaldehyde might acts as a precursor in the formation of these acetate species and that the presence of MoO_x also contributes to acetate formation.

Fig. 5 shows the results for the IR measurements after a sample of the Pd8Mo catalyst was exposed to a mixture of NO/ethanol at 573 K. Several bands were observed between 1200 and 1800 cm^{-1}. Fig. 5a shows the spectrum for this sample before being heated to 573 K, and bands around

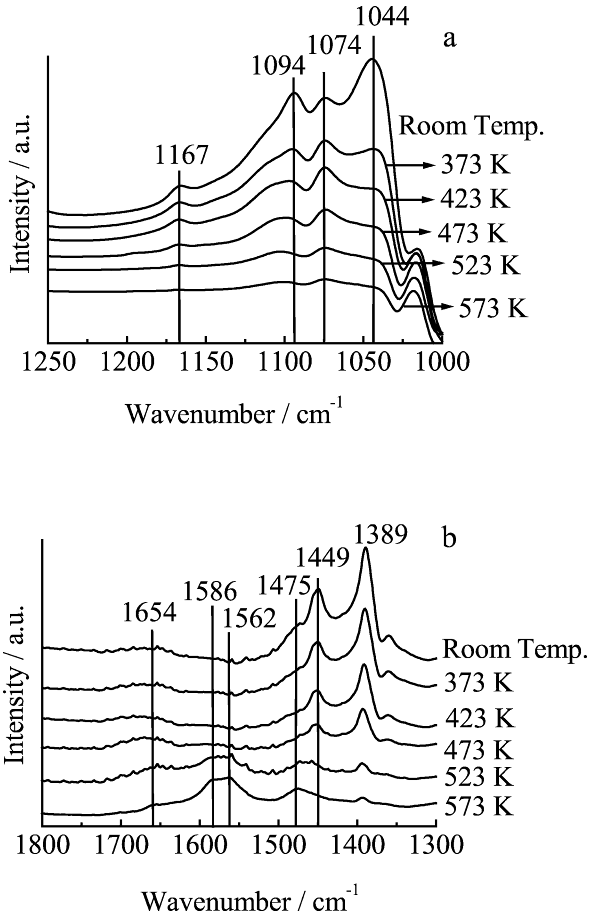

Fig. 4. IR spectra of adsorbed ethanol on Pd8Mo/Al_2O_3.

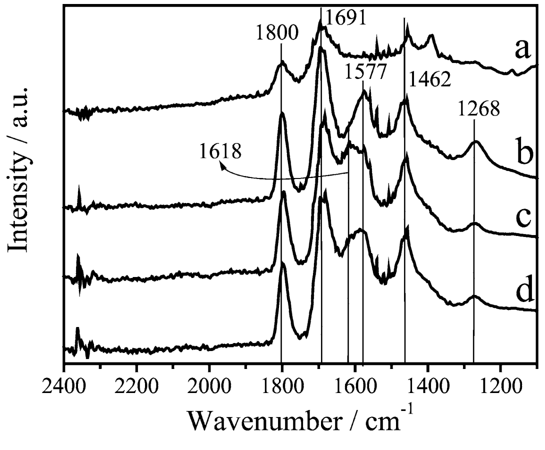

Fig. 5. IR spectra after exposure of Pd8Mo to NO + ethanol mixture at: (a) room temperature, (b) room temperature after being heated to 573 K, (c) sample in b after He flow, and (d) sample in c after vacuum.

1390, 1460, 1691, and 1800 cm^{-1} besides a small shoulder at 1715 cm^{-1} were observed, although the region between 1500 and 1620 cm^{-1} was not well resolved. The spectra presented in Figs. 5b–d were very similar, showing bands around 1268, 1462, 1577, 1690, and 1800 cm^{-1}.

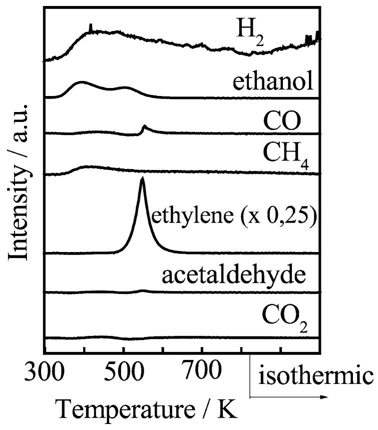

Fig. 6. TPD profile of ethanol adsorbed on Al_2O_3.

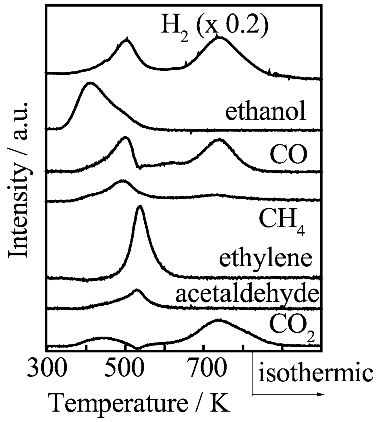

Fig. 7. TPD profile of ethanol adsorbed on Pd/Al_2O_3.

3.3. Ethanol temperature-programmed desorption

The TPD profiles after adsorption of ethanol on alumina and Pd/Al_2O_3 catalyst are presented in Figs. 6 and 7. Ethanol and ethylene were the main desorption products for the support. Ethanol desorbed in two peaks (395 and 500 K) while a great formation of ethylene was observed around 550 K.

The Pd/Al_2O_3 catalyst showed a decrease in ethylene production when compared to alumina. Besides that, three distinct features were observed: first, the formation of CO, CH_4, and H_2 (ethanol decomposition products) at 495 K, second, the formation of acetaldehyde at 530 K due to ethanol dehydrogenation; and finally, a further desorption of CO, H_2, and CO_2 was detected at higher temperatures (above 723 K).

Figs. 8 and 9 present the TPD profile after adsorption of ethanol on 8Mo and Pd8Mo catalysts. These results show a further decrease in ethylene formation (mainly on Pd8Mo). For the 8Mo catalyst, there was desorption of ethanol at 386 and 475 K, while for Pd8Mo, ethanol desorbed only at 405 K. The simultaneous formation of CO, CH_4, and H_2 around 475 K (in a similar way as the Pd/Al_2O_3 catalyst) was only observed for the Pd8Mo sample. In addition, CO, H_2, and CO_2 were also detected at high temperatures, not seen on 8Mo. Furthermore, both samples presented forma-

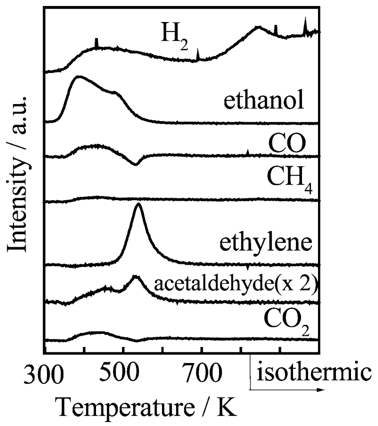

Fig. 8. TPD profile of ethanol adsorbed on 8Mo/Al_2O_3.

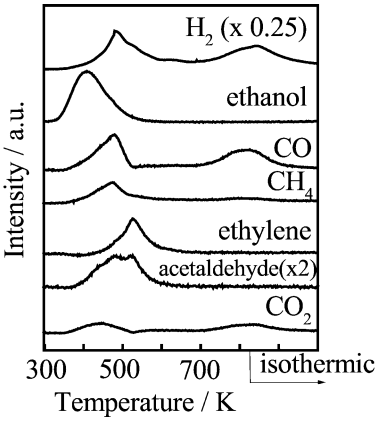

Fig. 9. TPD profile of ethanol adsorbed on Pd8Mo/Al_2O_3.

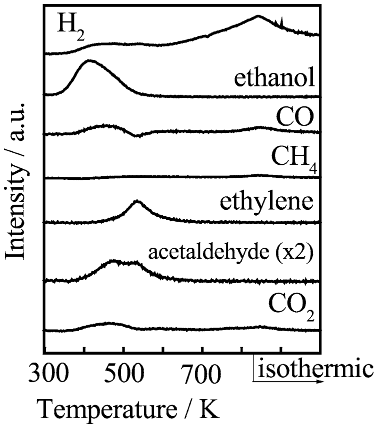

Fig. 10. TPD profile of ethanol adsorbed on 20Mo/Al_2O_3.

tion of acetaldehyde in two peaks (455 and 532 K for 8Mo and 479 and 522 K for Pd8Mo).

The TPD results after adsorption of ethanol on 20Mo and Pd–20Mo catalysts were very similar (Figs. 10 and 11). Both showed little formation of ethylene and the presence of two peaks corresponding to acetaldehyde around 473 and 520 K. Although not as intense as before, the desorption of CO, CO_2, and H_2 at higher temperatures could also be observed.

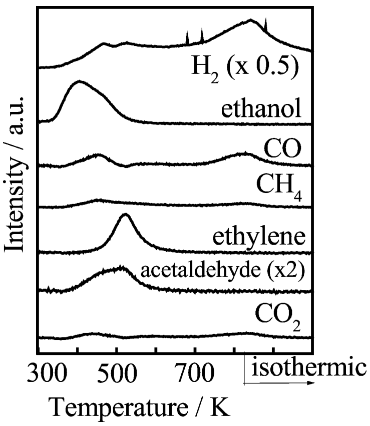

Fig. 11. TPD profile of ethanol adsorbed on Pd20Mo/Al_2O_3.

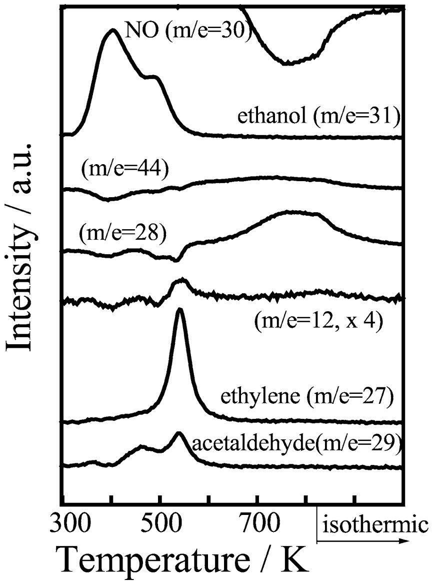

Fig. 12. NO + ethanol TPSR profile on 8Mo/Al_2O_3.

3.4. Temperature-programmed surface reaction

During TPSR measurements, some products were identified by secondary fragment signal in the mass spectrometer analysis. Since the signal $m/e = 28$ is attributed to both CO and N_2 (also a secondary fragment of CO_2), the signal used to distinguish one from the other, together with their main signals, was the CO secondary mass fragmentation signal $m/e = 12$. In the same way, the signal $m/e = 44$ may be related to CO_2 or N_2O and the use of secondary fragments ($m/e = 28$ and 12 for CO_2 and $m/e = 44$ and 30) were also needed.

TPSR results for the 8Mo catalyst are shown in Fig. 12. The profile is very similar to that observed for the TPD of adsorbed ethanol (Fig. 8) with ethylene formation around 540 K, two peaks of acetaldehyde at 465 and 535 K, and ethanol desorption at 400 and 490 K. NO consumption was observed only above 600 K in a wide temperature range

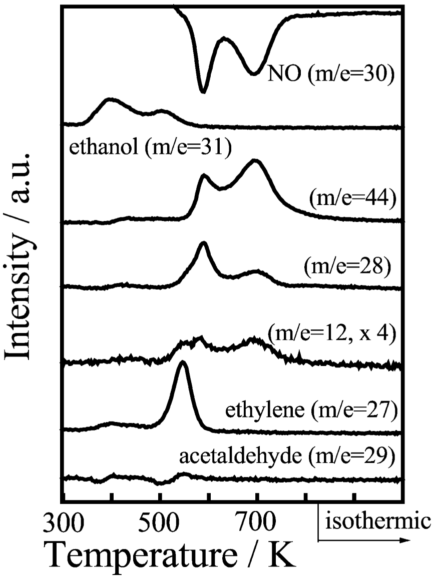

Fig. 13. NO + ethanol TPSR profile on Pd/Al_2O_3.

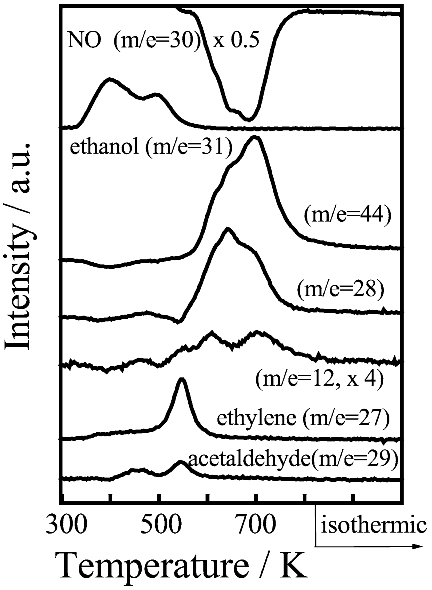

Fig. 14. NO + ethanol TPSR profile on Pd8Mo/Al_2O_3.

and together with the increase in intensity of the signals $m/e = 28$ and 44.

Figs. 13 and 14 show the TPSR profiles for Pd and Pd8Mo catalysts. On Pd/Al_2O_3, the results show the desorption of ethanol at 390 and 500 K and formation of ethylene at 545 K. Unlike the TPD results for this catalyst (Fig. 7), the simultaneous formation of CO, CH_4, and H_2 around 495 K was not observed and virtually no acetaldehyde was formed. A large consumption of NO was seen at 590 and 690 K, with the simultaneous increase of signals $m/e = 44$, 28, and 12.

For the Pd8Mo, ethanol desorption was observed at 400 and 490 K, with formation of ethylene at 545 K but, again, simultaneous CO, CH_4, and H_2 were not seen. Unlike the Pd/Al_2O_3 catalyst, a small amount of acetaldehyde was detected around 455 and 545 K. NO consumption began at slightly higher temperatures, showing a well-defined peak at 690 K and two small shoulders around 640 and 612 K. The NO consumption was followed by the simultaneous increase in the intensity of signals $m/e = 44$ and 28. On the other hand, the signal $m/e = 12$ (associated with CO and/or CO_2 formation) was seen only around 605 and 695 K.

3.5. Catalytic activity

Table 2 displays NO and ethanol conversion and selectivity values for each temperature on all samples. The 8Mo and 20Mo catalysts were inactive for NO conversion, but active for ethanol decomposition. Pd8Mo was more active for NO conversion than Pd20Mo catalyst; however, in this temperature range, the Pd/Al_2O_3 catalyst presented better NO conversion than the others. This behavior is different from the previous one for the NO + CO reaction [12], where the Pd–Mo-containing catalysts were more active. Nevertheless, at 593 K, the samples containing Pd showed similar NO conversion. Considering H_2 chemisorption results, it was possible to calculate the turnover frequency (TOF) over the exposed Pd sites for the Pd and Pd8Mo samples. The results obtained are very interesting and may be seen in Table 2. They show that the Pd–Mo catalyst presented higher values when compared to the Pd-only sample.

N_2 and N_2O were the only nitrogen-containing products observed for this reaction and regardless of the presence or amount of Mo, the selectivity for N_2 was approximately the same for all active samples. Once again, this result is quite different from previous NO + CO reaction [12], where the addition of Mo to Pd remarkably improved N_2 selectivity. Acetaldehyde was not observed for the Pd and Pd8Mo catalysts, while the other samples showed a high selectivity for this product. Note that the Pd/Al_2O_3 and 8% Mo-loading samples exhibited significant ethylene formation, while the 20% Mo-loading catalysts did not. Furthermore, no CO formation was seen on the Mo-only catalysts.

4. Discussion

The results presented above are a continuation of a line of work in which the alumina-supported Pd–Mo catalysts are being studied. Previously published papers [11–13] have thoroughly investigated the NO adsorption properties of these catalytic systems, which we find important and relevant for the discussion and conclusions drawn here. Therefore, before the discussion on the results presented in this work, we find it is suitable to describe some important points of our previous works regarding NO adsorption.

The previously published papers [11–13] studied the NO adsorption/decomposition properties on the Pd–Mo/Al_2O_3 surface using infrared as well as temperature-programmed desorption experiments. In a general sense, the TPD profiles for NO adsorption on Pd, Mo, and Pd–Mo catalysts

Table 2
Conversion and selectivity values for the NO + ethanol reaction

Catalyst	Temperature (K)	NO conversion (%)	TOF $(s^{-1})^a$	N_2 selectivity (%)	Ethanol conversion (%)	Selectivity of carbon species (%)			
						CO	CO_2	Acetald.	Ethyl.
Pd	523	0	0	–	–	–	–	–	
	553	20	0.91	72	78	5	33	0	62
	573	29	1.32	62	79	13	45	0	42
	593	49	2.34	66	85	11	44	0	45
Pd8Mo	523	0	0	–	55	30	61	0	9
	553	8	1.74	61	66	44	50	0	6
	573	34.5	7.50	67	74	38	47	0	15
	593	46	10.00	68	75	34.5	40.5	0	25
Pd20Mo	523	0	–	–	–	–	–	–	–
	553	0	–	–	51	0	56	44	0
	573	13	–	63	60	7	56	37	0
	593	45	–	67	71	11	51	26	16
8Mo	523	0	–	–	60	0	37	50	13
	553	0	–	–	69	0	47	29	23
	573	0	–	–	71	0	33	52	15
	593	0	–	–	78	0	42	32	25
20Mo	523	0	–	–	39	0	43	57	0
	553	0	–	–	48	0	29	71	0
	573	0	–	–	60	0	22	67	11
	593	0	–	–	70	0	7	80	13

Acetald., acetaldehyde; ethyl., ethylene.

[a] Mole of reacted NO/s ($\times 10^{25}$).

were quite different, indicating that NO interacts differently in each case. While on the Pd-only and 8Mo samples the formation of N_2 during TPD occurred only above 600 K (broad peaks), on the Pd–8Mo sample there was a sharp, intense peak of N_2 at 520 K (and another peak at 773 K). Besides lowering the temperature of N_2 formation (first peak), the presence of Pd and Mo on the Pd–Mo catalyst also increased the selectivity for N_2 during TPD, when compared to the other samples. According to the authors' discussion, the high temperature N_2 formation is attributed to inactive adsorbed nitrogen species (N_a species formed upon NO adsorption) which are strongly bounded and inhibit further NO adsorption and dissociation. The addition of molybdenum oxide to the palladium catalyst decreased the fraction of the inactive N_a species, thus promoting the NO dissociation to N_2 at lower temperatures. The authors further suggested that the increase in NO dissociation on the Pd–Mo catalyst could be due to the modification of the electronic properties of palladium in the presence of MoO_x species (they observed a decrease in adsorption strength of CO on Pd on the Pd–Mo catalyst). They concluded that the formation of new adsorption sites between Pd and MoO_x could be responsible for decreasing the stabilization of adsorbed nitrogen species on the surface of palladium.

4.1. Adsorption of ethanol

The high selectivity of alumina for the dehydration of ethanol to ethylene during TPD analyses (Fig. 6) agrees well with the work of McCabe and Mitchell [20], who attributed this to the presence of strong acid sites. Contrary to Cordi and Falconer [5], acetaldehyde or dehydrogenation products were not observed during TPD of adsorbed ethanol on alumina. The IR analyses of ethanol on alumina (Fig. 1) showed a decrease in intensity of the bands related to ethoxy species with increasing temperature. This suggests that part of the ethoxy species are desorbed as ethanol (Fig. 6) and part dehydrated to ethylene.

The Pd/Al_2O_3 catalyst significantly changed the product distribution during TPD analysis (Fig. 7) showing simultaneous formation of CO, CH_4, and H_2 at 495 K due to ethanol decomposition on Pd sites. However, the infrared analyses of ethanol adsorption on the Pd/Al_2O_3 catalyst (Fig. 2) was very similar (at low temperatures) to the Al_2O_3 support (Fig. 1), showing mainly the presence of ethoxy species adsorbed on alumina. These results suggest that the ethoxy species adsorbed on alumina migrate to the Pd particles and decompose. A similar result was reported by Cordi and Falconer [5] as they suggested that part of the ethanol adsorbed on alumina diffuses to the Pd sites, where decomposition occurs. In addition, according to them the α-carbon forms CO and the β-carbon forms CH_4 during ethanol decomposition.

Noteworthy is the formation of CO, CO_2, and H_2 at high temperatures. Cordi and Falconer [5] also observed this during TPD of adsorbed ethanol on Pd/Al_2O_3 catalysts and suggested that it might be due to the decomposition of a more stable carbon species formed during ethanol decomposition at lower temperatures. In fact, the infrared measurements (Fig. 2) indicated the formation of acetate species as the temperature was raised from 523 to 573 K, which is the same temperature range as acetaldehyde formation during TPD (Fig. 6). It is possible that while ethanol (adsorbed as ethoxy species) is dehydrogenated on Pd sites to form acetaldehyde, more stable acetate species are also formed. These species remain adsorbed and are the precursors for CO, CO_2, and H_2 production at high temperature. Cordi and Falconer [5] further suggested that a partial oxidation product from ethanol, such as acetaldehyde and/or acetic acid, might be the precursor for the more stable carbon species. However, no formation of acetic acid was observed in this work, indicating that acetaldehyde is probably the precursor for the acetate species.

For the catalysts containing Mo, there was a drastic reduction of ethylene formation, which is a reaction that is mainly catalyzed by the acid sites on the support. However, a large fraction of the alumina surface should be covered since a MoO_3 monolayer is usually formed between 8 and 12% Mo loading [12,19]. This result is supported by the infrared measurements of adsorbed ethanol on the 8% Mo-containing catalysts (Figs. 3 and 4), since the bands related to the ethoxy species adsorbed on alumina were less intense.

Another feature presented by the Mo-containing catalysts was that acetaldehyde formation exhibited two peaks during TPD (Figs. 8 and 9). The first one was only present on the catalysts containing molybdenum oxide and might be attributed to the oxidative dehydrogenation of ethanol adsorbed on the partially reduced molybdenum oxide. In fact, Iwasawa et al. [21] studied the reaction intermediates during ethanol oxidation over silica-supported molybdenum oxide catalysts using IR spectroscopy and in situ Raman spectroscopy. The authors observed bands which were attributed to the presence of adsorbed ethoxide structures. The in situ Raman spectroscopy measurements at reaction conditions identified two types of ethoxide species, which were associated with Mo=O and Mo–O–Mo sites. A very similar result was obtained by Zhang et al. [22] while studying ethanol oxidation over MoO_3/Al_2O_3 catalysts. According to both works, the ethoxide species bonded to a terminal oxygen group produced acetaldehyde, while the ethoxide species bonded to a bridging oxygen group produced ethylene, which agrees well with the results observed here.

On the other hand, the second peak of acetaldehyde formation (at a slightly higher temperature) was observed on all samples, with the exception of the support alone. One possible explanation for this would be the dehydrogenation of the ethoxy species initially adsorbed on alumina, which migrates to the active sites (MoO_x, in the case of the Mo catalysts; Pd^0 in the case of the Pd catalysts; and MoO_x or Pd^0, in the case of the Pd–Mo catalysts). The migration of such species could be the limiting step of the second acetaldehyde formation, thus occurring at higher temperature.

For the Pd8Mo catalyst, the simultaneous formation of CO, CO_2, and H_2 at 475 K (Fig. 9) was, once again, due to the decomposition of ethanol on Pd sites. However, despite the presence of Pd, the Pd20Mo catalyst did not show high selectivity for the decomposition of ethanol to CO, CH_4, and H_2 at low temperatures (Fig. 11). In fact, the TPD profile for the Pd20Mo catalyst was very similar to the TPD profile for the 20Mo catalyst (Fig. 10). The high concentration of Mo on these samples favors the presence of bulk MoO_3, as observed previously [12]. Therefore, this might indicate that bulk MoO_3 partially covers the Pd metallic sites, making it appear as if the presence of Pd had no direct effect on the properties of the Pd20Mo catalyst for the adsorption of ethanol. In addition, the covering of Pd particles by MoO_x species is supported by H_2 chemisorption results and it has also been reported in the literature [15,16].

The infrared analysis of adsorbed ethanol on the 8Mo and Pd8Mo catalysts showed bands at 1662–1654, 1562–1566, 1586, and 1475 cm^{-1} as the samples were heated. The first group of bands was possibly associated with acetate species on MoO_x while the second group was attributed to acetate species on alumina. When comparing the Pd-free samples with the ones containing Pd, it becomes evident that the presence of Pd favors the formation of acetate species, although the presence of MoO_x species also contributes to this. Furthermore, the acetate species are formed at the same temperature range as acetaldehyde is produced during TPD analysis, thus suggesting that acetaldehyde might be the precursor of the formation of such species. Once again, it seems that, since these species are more stable, they remain adsorbed until they decompose at higher temperatures (above 723 K), originating CO, CO_2, and H_2 as seen on the TPD profiles.

A final and important issue regarding the adsorption properties of ethanol on the catalysts studied here may be pointed out by comparing the TPD profiles of the Pd, Mo, and Pd–Mo catalysts. When looking at the Pd–Mo TPD results and comparing these to their respective Pd-free or Mo-free pair (for example, Pd8Mo compared to Pd/A_2O_3 and/or to 8Mo), there are clearly no new or distinct features arriving from a possible Pd–Mo interaction. All features observed on the bimetallic samples are either attributable to the presence of Pd, MoO_x, or alumina. Although Pd is in close contact and interacts with molybdenum suboxide species as observed in previous studies by TPR and CO infrared measurements [13], this apparently has no effect on the adsorption/dissociation properties of ethanol. This is in contrast to what was observed previously for the adsorption/dissociation properties of NO [11,13], since the presence of closely associated Pd and MoO_x considerably changed NO dissociation and product distribution during TPD of adsorbed NO.

4.2. Ethanol + NO reaction

The NO + ethanol temperature-programmed surface reaction for the 8Mo catalyst (Fig. 12) was very similar to the ethanol TPD profile (Fig. 8), showing the same ethanol desorption/decomposition pattern for temperatures below 600 K. Apparently, the presence of NO had no influence on the adsorption properties of ethanol on the reduced molybdenum oxide. NO consumption was observed only above 600 K, together with the increase of intensity of signals

$m/e = 28$ and 44 (very weak), indicating the formation of both N_2 (main product) and N_2O. Since the intensity of the signal $m/e = 12$ did not increase, no CO or CO_2 was produced above 600 K, thus showing that NO decomposition on the partially reduced molybdenum oxide surface was the only event contributing to NO consumption. In other words, the reaction between flowing NO and adsorbed ethanol or acetate species did not take place. In a previous work [13], TPD measurements of adsorbed NO on this catalyst showed simultaneous formation of N_2 and N_2O only above 600 K, which agrees with the results observed here. These observations suggest that neither NO or ethanol directly compete for adsorption sites on the partially reduced molybdenum oxide surface.

The TPSR measurements for the Pd-containing catalysts (Figs. 13 and 14) showed rather similar characteristics and the discussion that will be carried on for the Pd/Al_2O_3 sample will later be referenced by the discussion on the Pd8Mo sample.

When comparing the TPD profile of adsorbed ethanol (Fig. 7) with the TPSR results for the Pd/Al_2O_3 catalyst, some important features may be pointed out. First, during TPD, only one ethanol desorption peak was observed (around 395 K), whereas for the TPSR there were two peaks (at 390 and 500 K). The simultaneous formation of CO, CO_2, and H_2 at 495 K seen during TPD was not observed on the TPSR profile. As discussed above, such product formation around 500 K (for TPD) was due to the decomposition of ethanol (originally adsorbed on alumina as an ethoxy specie) on Pd particles. For some reason, during TPSR the adsorbed ethanol is not allowed to decompose on the Pd sites and instead it simply desorbs as unreacted ethanol (hence the second ethanol peak at 500 K during TPSR) in exactly the same way as was seen for the TPD profile on alumina (Fig. 6). It suggests that when NO is present, the NO molecules readily adsorb on the Pd sites, removing and/or not allowing ethanol adsorption nor reaction on the metallic particles. McCabe and Mitchell [20] studied the direct oxidation of ethanol on alumina-supported Pd and Pt catalysts and observed that the presence of NO inhibited the catalytic activity. They attributed this to the fact that the NO molecules adsorbed more strongly than ethanol on the metallic sites. For the same reason as discussed above, almost no acetaldehyde was formed during TPSR on Pd/Al_2O_3.

Two well-defined NO consumption peaks were observed with the simultaneous increase in the intensities of the signals $m/e = 44$, 28, and 12. The signals $m/e = 28$ may be attributed to either N_2, CO, or both while the signal $m/e = 44$ may be related to N_2O, CO_2, or both. However, the increase in intensity of the signal $m/e = 12$ is indicative of the formation of CO and/or CO_2, revealing that NO reacts with adsorbed carbon-containing species. On the other hand, the IR results showed that at the temperature range in which such reaction took place during TPSR, only acetate species were present, suggesting that these are the carbon-containing species that react with NO.

For the Pd8Mo catalyst, the TPSR results also indicated that NO adsorption on the Pd particles hindered ethanol decomposition since there were two ethanol desorption peaks and the absence of the ethanol decomposition products (CO, CH_4, and H_2). On the other hand, there were two distinct peaks of acetaldehyde formation at the same temperature as observed during TPD (Fig. 9), attributed to the oxidative dehydrogenation of ethanol on the partially reduced molybdenum oxide. Once again, this shows that the presence of NO does not modify the adsorption properties of ethanol on MoO_x.

NO consumption began only above 500 K, with the increase of intensity of the signals $m/e = 44$, 28, and 12. However, unlike the Pd/Al_2O_3 catalyst, one NO consumption peak (690 K) and two shoulders (640 and 612 K) could be identified, but only the peak at 690 K and the shoulder at 612 K were followed by the increase of intensity of the signal $m/e = 12$ (695 and 605 K), indicating that the reaction between NO and adsorbed acetate species occurred around 690 and 610 K. These are approximately the same temperatures at which the reaction takes place during TPSR on Pd/Al_2O_3, which indicates that the reaction proceeds in the same way on both catalysts. That is, the reaction between NO and adsorbed acetate species probably follows the same pathway and apparently the presence of closely associated Pd–MoO_x does not originate new reaction sites for this reaction. Furthermore, the TPSR results for the 8Mo sample showed that the MoO_x species alone do not promote the reaction between adsorbed carbon species and NO. All of this suggests that such reaction occurs at the Pd–alumina or Pd–MoO_x interface. The NO consumption peak at 640 K is most possibly due to the dissociation of NO on MoO_x with the formation of both N_2 ($m/e = 28$) and N_2O ($m/e = 44$), and it seems to have no influence on the NO + ethanol reaction.

The catalytic activity measurements (Table 2) showed that Pd/Al_2O_3 was the most active catalyst for NO conversion. This is in contrast with the previously studied NO + CO reaction [12] on the same catalysts. For the NO + CO reaction system, the addition of Mo to the Pd/Al_2O_3 catalyst improved NO conversion and this was explained by a redox mechanism in which NO adsorbed and dissociated on the partially reduced molybdenum oxide surface and the oxygen atom from NO was made available for the oxidation of CO on Pd. Apparently, the NO + ethanol reaction on these catalysts occurs through a different reaction pathway.

The NO conversion pattern for the reaction studied here was as follows: $Pd/Al_2O_3 > Pd8Mo > Pd20Mo > 8Mo$ and 20Mo (no activity). This suggests that as Mo is added, the activity for NO reduction with ethanol diminishes. On the other hand, it was seen [12] that as the amount of Mo increases, a monolayer of molybdenum oxide is formed and after that, bulk MoO_3 is present. Through the ethanol TPD results, it was seen that MoO_x might cover part of the Pd particles and this, of course, is more evident on the Pd20Mo sample. In addition, hydrogen chemisorption results showed less exposed Pd particles when Mo is present. In fact, the covering of Pd particles by MoO_x suboxide species has been reported in the literature, even at low Mo loadings [15]. Such effect of the presence of Mo may be responsible for the activity drop on the Pd–Mo catalysts. In other words, it seems that for this reaction, it is very important that the metallic sites are exposed. This was not true for the NO + CO reaction, since the Pd20Mo catalyst was more active than the Pd/Al_2O_3 catalyst [11]. Such great differences from one reaction to another called our attention and in order to explain the results obtained here, a comparison with the NO + CO reaction studied before [11,12] will be made.

As noted above, for the NO + CO reaction the addition of Mo to the Pd catalyst changed the prevailing reaction mechanism and a new redox mechanism was proposed where NO adsorbed and reacted on the MoO_x surface, while CO was oxidized on the Pd particles. According to this mechanism, NO conversion is enhanced by the presence of Pd–MoO_x in a bifunctional-type mechanism. On the other hand, for the NO + ethanol reaction, it seems that the Pd particles have to be exposed, which indicates that the main reaction step must take place on the metallic sites or at the metal/oxide interface, as suggested by TPSR results. In addition, the N_2 selectivity was approximately the same on all samples, indicating that the reaction mechanism is probably the same, regardless of the presence of Mo (for the NO + CO reaction, N_2 selectivity was higher on the Mo-containing catalysts). Nevertheless, the fact that the selectivity was the same could also mean that the reaction was at the equilibrium point. However, thermodynamical calculations were made for this system and this possibility was discarded. Furthermore, TPSR analysis also suggested that the reaction pathway was the same on all Pd-containing catalysts.

As discussed above, the TPSR results showed that for this reaction system the NO molecules adsorb preferentially on the Pd sites, while ethanol adsorbs either on the partially reduced molybdenum oxide surface and/or the support. This is in total contrast with what happened during the redox mechanism for the CO + NO reaction, where CO mainly adsorbed on Pd and NO on the MoO_x species, suggesting, once again, that a similar redox mechanism for the NO + ethanol reaction is unlikely and that the main reaction step occurs on the Pd particles. Besides that, the TPSR analyses, together with the IR and TPD results, also indicated that NO probably reacts with the acetate species (formed above 450 K) which are adsorbed on the Al_2O_3 and/or the MoO_x surface and that such reaction takes place at the metal/oxide interface.

However, an interesting result was obtained when the turnover frequency was calculated (Table 2). By assuming that the NO conversion is dependent on the exposed Pd and using the H_2 chemisorption results as an estimate of exposed Pd particles, it was possible to calculate the TOF over exposed Pd sites for the Pd and Pd8Mo catalysts. These values were much higher when Mo was present, indicating that although MoO_x in close contact with Pd hampers overall NO conversion, it somehow enhanced the reaction rate at the metal oxide interface.

Other important results that must be noted are the fact that ethylene formation was seen on all samples and that the selectivity for its formation was higher on the catalysts with more exposed alumina surface. Indeed, the dehydration of ethanol to ethylene is a characteristic reaction on alumina (also observed during TPD experiments) and this is a side reaction that occurs simultaneously with the NO + ethanol reaction, thus contributing to ethanol conversion.

Acetaldehyde formation was observed on all samples except for the Pd/Al_2O_3 and Pd8Mo, which were the most active catalysts for NO conversion. According to the TPD and IR results, it seems that acetaldehyde formation is an important step for originating more stable acetate species and it is believed that these species react with adsorbed NO during TPSR. Apparently, the formation of acetaldehyde is a necessary step for reaction to take place. Since no acetaldehyde was detected for the more active catalysts, it seems that acetaldehyde might be an intermediate product during the reaction process and that its formation (dehydrogenation of ethanol) should be the limiting step. In other words, as soon as dehydrogenation of ethanol occurs, the acetaldehyde intermediate readily originates the acetate species, which immediately react with the adsorbed NO, thus explaining the absence of acetaldehyde on the most active catalysts.

Some works dealing with the oxidation of ethanol by oxygen (much more potent oxidation agent than NO) have shown that the activation of ethanol is the rate-determining step. Zhang et al. [22] studied the oxidation of ethanol on supported molybdenum oxide catalysts using in situ infrared and Raman measurements. They observed that the acetaldehyde formation on such catalysts occurred in two steps: the first would be the adsorption of ethanol with formation of ethoxy species while the second, rate-limiting step, would be the decomposition of these species to acetaldehyde. Nagal and Gonzales [18] studied the oxidation of ethanol and acetaldehyde on Pt/SiO_2 catalysts using in situ infrared analyses and according to their observations, they proposed a reaction mechanism in which the dehydrogenation of an adsorbed ethoxy species would be the limiting step. These dehydrogenated species could than be oxidized to form intermediate acetate species that would react originating CO_2. According to the authors, the formation of acetate species also occurs via acetaldehyde formation, as follows:

$$\underset{\text{Ethanol}}{CH_3CH_2OH} \xrightarrow{S} \underset{\text{Ethoxy}}{CH_3CH_2O\text{–}S} \rightarrow H_2 + \underset{\text{Acetaldehyde}}{CH_3CHO}$$

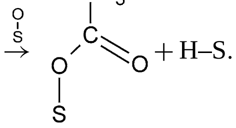

Acetate species

Some works have investigated the NO reduction by alcohols [10,23–25]. Noto et al. [23] studied the reduction of NO_x by ethanol on silver-based catalysts and found that NO_x is reduced after ethanol is oxidized to acetaldehyde and, furthermore, when oxidized or partially oxidized products are formed by acetaldehyde oxidation, thus showing that acetaldehyde formation is an important step in this reaction. Toops et al. [10] studied the reduction of NO by methanol over La_2O_3 and based on kinetic data, they suggested a mechanism involving two types of adsorption sites, as follows:

$$6[\mathrm{NO} + \mathrm{S} \leftrightarrows \mathrm{NO{-}S}],$$

$$2[\mathrm{CH_3OH} + * \leftrightarrows \mathrm{CH_3OH{-}*}],$$

$$2[\mathrm{NO{-}S} + \mathrm{CH_3OH{-}*} \rightarrow \mathrm{HNO{-}S} + \mathrm{CH_3O{-}*}]$$

rate-determining step,

$$4\mathrm{NO{-}S} + 2\mathrm{HNO{-}S} + 2\mathrm{CH_3O{-}*} \leftrightarrows 3\mathrm{N_2} + 4\mathrm{H_2O} + 2\mathrm{CO_2} + 6\mathrm{S} + 2*.$$

According to the authors, the rate-determining step involves the reaction between adsorbed NO and adsorbed methanol, originating methoxy species. Based on their observations, they have discarded the possibility of methanol decomposition to CO and H_2 with these compounds then reacting with adsorbed NO. Although the rate-determining step would involve the methanol molecule, they have not investigated the possible adsorption intermediates involved during adsorption of methanol, such as the formation of formate species. Several works in the literature have reported formate species formation upon methanol adsorption at high temperatures [26–28] and this could possibly be an important reaction intermediate involved in the rate-determining step.

In this work, we believe that the ethanol + NO reaction occurs similarly to what was proposed by Toops et al. [10] for the methanol + NO reaction, except that according to the results obtained here and discussed above, we find there is evidence to suggest that acetate species are an important reaction intermediate and that its formation is linked to the dehydrogenation of ethanol to acetaldehyde. We also believe that there are two adsorption sites for NO (Pd particles) and ethanol (Al_2O_3 and/or MoO_x) and that the reaction between the involved species occurs at the metal/oxide interface.

Based on what was discussed above, a possible reaction mechanism was proposed for this system.

First, NO adsorbs preferentially on Pd particles while ethanol adsorbs dissociatively forming adsorbed ethoxy species:

$$10[\mathrm{NO} + \mathrm{Pd} \rightarrow \mathrm{NO{-}Pd}], \tag{1}$$

$$2[\mathrm{CH_3CH_2OH} + 2\mathrm{S} \rightarrow \mathrm{CH_3CH_2O{-}S} + \mathrm{H{-}S}]. \tag{2}$$

At the reaction temperature, these ethoxy species are dehydrogenated, providing the overall dehydrogenation of ethanol to acetaldehyde:

$$2[\mathrm{CH_3CH_2O{-}S} + \mathrm{H{-}S} \rightarrow \mathrm{CH_3CHO} + \mathrm{H_2} + 2\mathrm{S}]. \tag{3}$$

Once again, at the reaction temperature, acetaldehyde is readily activated originating intermediate acetate species:

$$2[\mathrm{CH_3CHO} + \mathrm{S} + \mathrm{NO{-}Pd} \xrightarrow{[\mathrm{O}]} \mathrm{CH_3COO{-}S} + \mathrm{HNO{-}Pd}]. \tag{4}$$

Reaction between adsorbed species then proceeds at the metal/oxide interface:

$$8\mathrm{NO{-}Pd} + 2\mathrm{HNO{-}Pd} + 2\mathrm{CH_3COO{-}S} \xrightarrow{-[\mathrm{O}]} 5\mathrm{N_2} + 2\mathrm{CO_2} + 4\mathrm{H_2O} + 2\mathrm{S} + 10\mathrm{Pd}, \tag{5}$$

where [O] represents surface oxygen.

Some considerations must be made regarding other surface reactions. As shown by the results presented before, a side reaction may also occur during NO reduction by ethanol, which is the dehydration of ethanol to ethylene on the alumina surface, thus contributing to ethanol conversion:

$$\mathrm{CH_3CH_2O{-}S} + \mathrm{H{-}S} \rightarrow \mathrm{C_2H_4} + \mathrm{H_2O} + 2\mathrm{S}. \tag{6}$$

Although reaction (5) shows total oxidation products, the partial oxidation of adsorbed acetate species may also take place and in fact, product distribution during catalytic measurements did show the presence of both CO and N_2O.

According to the reaction mechanism proposed above and to the results presented in Table 2, it may be seen that since no acetaldehyde was formed on the Pd and Pd8Mo catalysts, it is suggested that reaction (3) must be the limiting step on this mechanism. That is, as soon as acetaldehyde is formed, it is converted into acetate species which then react with the adsorbed NO species. On the other hand, there was acetaldehyde formation on the Pd20Mo and this may be explained by the fact that for this sample, a large fraction of the Pd particles are covered by MoO_x (due to the high concentration of Mo), as discussed above, thus hampering steps 1 and 5 and allowing acetaldehyde to be formed. In other words, for this sample, not all of the acetaldehyde formed during reaction (3) is converted in reactions (4) and (5). Nevertheless, as the temperature is raised and the NO conversion increases, acetaldehyde selectivity considerably drops and this is better observed when comparing the selectivity values of samples Pd20Mo and 20Mo at 593 K.

These observations suggest that there are possibly two different processes affecting the overall reaction. The first would be the need for exposed Pd particles and its contact with MoO_x species while the second would be the ability to favor the dehydrogenation step [reaction (3)], which is rate determining. This is better understood by comparing the NO conversion data with TOF results. The turnover frequency was calculated as the NO conversion rate over Pd sites and by doing this we consider only the exposed Pd particles, thus eliminating the effect of Pd decoration by MoO_x. In this case, TOF numbers indicate that as the amount of MoO_x increases, so does the reaction rate at the metal/oxide interface. This could be explained by looking at the reaction mechanism proposed above. According to the mechanism and to the discussion presented before, acetaldehyde formation is a critical step in the reaction pathway since it is a precursor in originating acetate species. On the other hand, both TPD and TPSR measurements showed that when MoO_x was present, acetaldehyde formation was favored when compared to the Pd/Al_2O_3 sample, since two peaks of acetaldehyde were observed on the Mo-containing catalysts while just one peak was seen on the Pd-only catalyst during TPD. In other words, the MoO_x species were active for the dehydration of ethanol to acetaldehyde, while alumina was not. Furthermore, acetaldehyde formation during TPD on the Mo-containing catalysts began at lower temperatures than on Pd-only catalysts. Since it was seen that Pd particles and MoO_x are in close contact [12,13], and that acetaldehyde formation [reaction (3)] on MoO_x is favored, it would be reasonable to think that the reaction rate between NO and acetate species at the Pd–MoO_x interface would be favored over the Pd–Al_2O_3 interface, thus explaining the higher TOF numbers for the Mo-containing catalysts.

Nevertheless, when we look at the NO conversion results, we clearly see that the presence of exposed Pd particles are an important factor to be taken into account. For the Pd20Mo catalyst, for example, the amount of exposed Pd particles is very low (as seen by H_2 chemisorption), while the amount of MoO_x species is very large, so even though the MoO_x favors step 3 on the reaction mechanism, the reaction rate at the Pd–MoO_x interface is not high enough to account for acetaldehyde formation on MoO_x (which is achieved only at higher temperatures).

As an attempt to support the proposed mechanism, an additional IR measurement was performed on a sample of the Pd8Mo catalyst that was exposed to a mixture of NO/ethanol at reaction temperature. The results are displayed in Fig. 5.

Although it is difficult to establish band identifications since there may be overlapping of bands related to different adsorbed species, some considerations may still be made. Fig. 5a shows the IR result after the sample was exposed to the NO/ethanol mixture, but prior to heating and only bands around 1800 and 1691 cm^{-1} as well as the bands at 1390 and 1455 cm^{-1} were observed. According to the literature [11–13,29], NO adsorption on partially reduced molybdenum oxide originates absorption bands around 1815 and 1710 cm^{-1}(symmetric and antisymmetric stretching vibration modes, respectively) and therefore, the bands observed here at 1800 and 1691 cm^{-1} are most probably due to the adsorption of NO on MoO_x species. The bands at 1390 and 1455 cm^{-1} were also observed after adsorption of ethanol on Pd8Mo (Fig. 3) and were associated with ethoxy species on alumina. The region between 1500 and 1620 cm^{-1} was not well resolved.

Several works [30–32] have also identified different NO adsorption bands on Pd-based catalysts in the same region. Hoost et al. [30] studied the adsorption of NO on reduced Pd–Mo catalysts and they observed bands which were attributed to NO adsorbed on Pd(111) at 1740 and 1550 cm^{-1} and NO adsorbed on Pd(100) at 1670 cm^{-1}. In another work, Hoost et al. [31] investigated the adsorption of NO on Pd/alumina catalysts and identified three absorption regions as follows: 1753–1750 cm^{-1} (linear), 1615–1599 cm^{-1} (twofold bridged), and 1580–1572 cm^{-1} (threefold bridged), where the linear form was favored when the samples were reduced. However, in a previous work [13] the adsorption of NO on the Pd/Al_2O_3 and Pd–Mo/Al_2O_3 catalysts was studied using IR analyses and only a very weak absorption band at 1775 cm^{-1} (assigned to linearly adsorbed NO on Pd) was observed and this was attributed to the poor Pd dispersion presented by these catalysts. In fact, the Pd dispersion for the Pd/Al_2O_3 catalyst was only 23% and in addition to this, part of the Pd particles are covered by Mo species on the Pd8Mo sample and therefore, it was virtually impossible to identify the NO adsorption band on Pd in the results presented in Fig. 5.

Nevertheless, the results obtained after the sample was heated up to 573 K and cooled to room temperature (Figs. 5b and 5c after He flow and Fig. 5d after vacuum) showed, besides increased intensity of the bands related to NO adsorbed on MoO_x, the appearance of intense bands at 1577 and 1462 cm^{-1}. These new bands are at the same position as the acetate bands observed after ethanol adsorption, except that in this case, they were much more intense, thus evidencing the participation of such adsorbed intermediates in the reaction mechanism.

5. Conclusion

The TPD and IR measurements showed that ethanol adsorbs as ethoxy species and that as the surface is heated, more stable acetate species are formed and decompose only at higher temperatures. The results further suggest that acetaldehyde (ethanol dehydrogenation product) is an important precursor in the formation of such acetate species, which were identified on both Pd/Al_2O_3 and Pd–Mo catalysts. However, the presence of Pd seems to favor their formation.

The TPSR as well as the catalytic tests results showed that partially reduced molybdenum oxide has no activity for the reduction of NO with ethanol and that such reaction occurs only in the presence of Pd. Furthermore, the TPSR analyses together with the TPD and IR measurements indicated that NO preferentially adsorbs on the Pd particles, while ethanol selectively adsorbs on alumina and/or partially reduced molybdenum oxide (MoO_x). In addition, the comparison of the TPSR results with TPD and IR suggested that NO reacts with adsorbed acetate species and that such reaction would occur at the metal/oxide interface.

The catalytic tests also showed that the addition of molybdenum oxide to the palladium catalyst decreased the activity for NO conversion, indicating that the main reaction step should take place at the Pd sites. In other words, it is important, for this reaction, that Pd particles are exposed. Nevertheless, the selectivity for N_2 formation was similar on all active samples, suggesting that the reaction mechanism is the same, independently of the presence of Mo. This was in striking contrast with the previously studied NO reduction with CO on these catalysts. Furthermore, since no acetaldehyde formation was observed for the more active catalysts and since acetaldehyde is an important intermediate in the formation of acetate species, the dehydrogenation of ethanol to acetaldehyde should be the rate-limiting reaction step.

In accordance with this, a new reaction mechanism was proposed where NO adsorbs on Pd particles and adsorption of ethanol on the support and/or MoO_x give rise to acetate species which may decompose and/or react with the NO molecules at the metal/oxide interface. Indeed, an IR measurement after exposure of Pd8Mo to a NO/ethanol mixture clearly revealed the presence of acetate species at reaction conditions. On the other hand, TOF results over exposed Pd particles showed that the presence of MoO_x enhanced the reaction rate at the metal/oxide interface, which was explained by the fact that such partially reduced molybdenum oxide species are in intimate contact with Pd and they favor the dehydrogenation of ethanol to acetaldehyde (probably the rate-determining step), as observed by TPD and TPSR analysis. Finally, we called attention to two important factors effecting the NO conversion. The first is the covering of Pd particles by MoO_x species while the second is the dehydrogenation of ethanol to acetaldehyde.

Acknowledgments

We thank CAPES for the scholarship (L.F.M.), and CNPq for financial support.

References

[1] J.N. Armor, Appl. Catal. B 1 (1992) 221.
[2] D.A. Guerrieri, P.J. Caffrey, V. Rao, SAE paper 950777, 85, 1995.
[3] A.P. Altshuller, Atmos. Environ. 27A (1993) 21.
[4] V.I. Pârvulescu, P. Grange, B. Delmon, Catal. Today 46 (1998) 233.
[5] E.M. Cordi, J.L. Falconer, J. Catal. 162 (1996) 104.
[6] H. Idriss, C. Diagne, J.P. Hindermann, A. Kiennemann, M.A. Barteau, J. Catal. 155 (1995) 219.
[7] A. Yee, J. Morrison, H. Idriss, J. Catal. 186 (1999) 279.
[8] Y. Ukisu, T. Miyadera, A. Abe, K. Yoshida, Catal. Lett. 37 (1996) 265.
[9] T. Miyadera, Appl. Catal. B 2 (1993) 199.
[10] T.J. Toops, A.B. Walters, M.A. Vannice, Catal. Lett. 64 (2000) 65.
[11] M.A.S. Baldanza, L.F. de Mello, A. Vannice, F.B. Noronha, M. Schmal, J. Catal. 192 (2000) 64.
[12] M. Schmal, M.A.S. Baldanza, M.A. Vannice, J. Catal. 185 (1999) 138.
[13] F.B. Noronha, M.A.S. Baldanza, M. Schmal, J. Catal. 188 (1999) 270.
[14] J.E. Benson, H.S. Hwang, M. Boudart, J. Catal. 30 (1973) 46.
[15] L.W. Konopny, A. Juan, D.E. Damiani, Appl. Catal. B 15 (1998) 115.
[16] G.M. Tonetto, M.L. Ferreira, D.E. Damiani, J. Mol. Catal. A 193 (2003) 121.
[17] R.G. Greenler, J. Chem. Soc. 82 (1962) 2488.
[18] M. Nagal, R.D. Gonzalez, Ind. Eng. Chem. Prod. Res. Dev. 24 (1985) 525.
[19] I. Halasz, A. Brenner, M. Shelef, Appl. Catal. B 2 (1993) 131.
[20] R.W. McCabe, P.J. Mitchell, Ind. Eng. Chem. Prod. Catal. Dev. 23 (1984) 196.
[21] Y. Iwasawa, Y. Nakano, S. Ogasawara, J. Chem. Soc., Faraday Trans. 74 (1978) 2986.
[22] W. Zhang, A. Desikan, S.T. Oyama, J. Phys. Chem. 99 (1995) 14478.
[23] T. Noto, T. Murayama, S. Tosaka, Y. Fujiwara, Soc. Automotive Eng. SP-1626 (2001) 45–52.
[24] T. Chafik, S. Kameoka, Y. Ukisu, T. Miyadera, J. Mol. Catal. A 136 (1998) 203.
[25] S. Kameoka, Y. Ukisu, T. Miyadera, Chem. Phys. 2 (3) (2000) 367.
[26] G.C. Cabilla, A.L. Bonivardi, M.A. Baltanas, J. Catal. 201 (2001) 213.
[27] E. Finocchio, M. Daturi, C. Binet, J.C. Lavalley, G. Blanchard, Catal. Today 52 (1999) 53.
[28] N. Narishige, M. Niwa, Catal. Lett. 71 (2001) 63.
[29] L. Portela, P. Grange, B. Delmon, Catal. Ver. Sci. Eng. 37 (4) (1995) 699.
[30] T.E. Hoost, G.W. Graham, M. Shelef, O. Alexeev, B.C. Gates, Catal. Lett. 33 (1996) 57.
[31] T.E. Hoost, K. Otto, K.A. Laframboise, J. Catal. 155 (1995) 303.
[32] M. Valden, R.L. Keiski, N. Xiang, J. Pere, J. Aaltonen, M. Pessa, T. Maunula, A. Savimäki, A. Lahti, M. Härkönen, J. Catal. 161 (1996) 614.